Chemical Research in Toxicology

Article

pubs.acs.org/crt

Replication Bypass of the *trans*-4-Hydroxynonenal-Derived (6*S*,8*R*,11*S*)-1,N^2-Deoxyguanosine DNA Adduct by the *Sulfolobus solfataricus* DNA Polymerase IV

Surajit Banerjee,[†] Plamen P. Christov, Albena Kozekova, Carmelo J. Rizzo, Martin Egli, and Michael P. Stone*

Departments of Chemistry and Biochemistry, Center in Molecular Toxicology, Vanderbilt Institute of Chemical Biology and the Vanderbilt-Ingram Cancer Center, Vanderbilt University, Nashville, Tennessee 37235, United States

Supporting Information

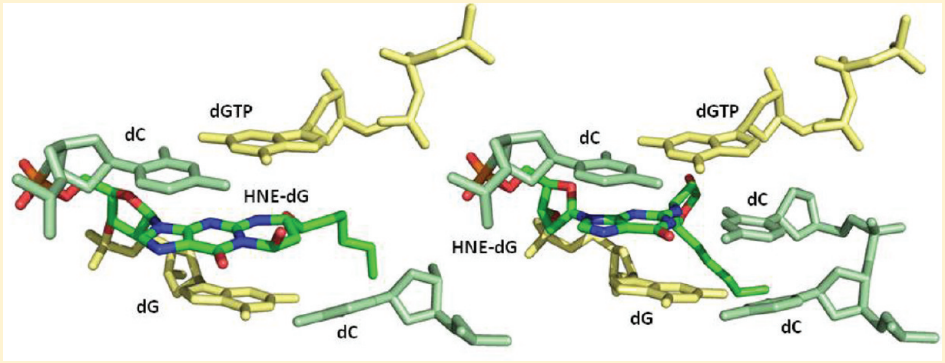

ABSTRACT: *trans*-4-Hydroxynonenal (HNE) is the major peroxidation product of *ω*-6 polyunsaturated fatty acids in vivo. Michael addition of the N^2-amino group of dGuo to HNE followed by ring closure of N1 onto the aldehyde results in four diastereomeric 1,N^2-dGuo (1,N^2-HNE-dGuo) adducts. The (6*S*,8*R*,11*S*)-HNE-1,N^2-dGuo adduct was incorporated into the 18-mer templates 5′-d(TCATXGAATCCTTCCCCC)-3′ and d(TCACXGAATCCTTCCCCC)-3′, where X = (6*S*,8*R*,11*S*)-HNE-1,N^2-dGuo adduct. These differed in the identity of the template 5′-neighbor base, which was either Thy or Cyt, respectively. Each of these templates was annealed with either a 13-mer primer 5′-d(GGGGGAAGGATTC)-3′ or a 14-mer primer 5′-d(GGGGGAAGGATTCC)-3′. The addition of dNTPs to the 13-mer primer allowed analysis of dNTP insertion opposite to the (6*S*,8*R*,11*S*)-HNE-1,N^2-dGuo adduct, whereas the 14-mer primer allowed analysis of dNTP extension past a primed (6*S*,8*R*,11*S*)-HNE-1,N^2-dGuo:dCyd pair. The *Sulfolobus solfataricus* P2 DNA polymerase IV (Dpo4) belongs to the Y-family of error-prone polymerases. Replication bypass studies in vitro reveal that this polymerase inserted dNTPs opposite the (6*S*,8*R*,11*S*)-HNE-1,N^2-dGuo adduct in a sequence-specific manner. If the template 5′-neighbor base was dCyt, the polymerase inserted primarily dGTP, whereas if the template 5′-neighbor base was dThy, the polymerase inserted primarily dATP. The latter event would predict low levels of Gua → Thy mutations during replication bypass when the template 5′-neighbor base is dThy. When presented with a primed (6*S*,8*R*,11*S*)-HNE-1,N^2-dGuo:dCyd pair, the polymerase conducted full-length primer extension. Structures for ternary (Dpo4-DNA-dNTP) complexes with all four template-primers were obtained. For the 18-mer:13-mer template-primers in which the polymerase was confronted with the (6*S*,8*R*,11*S*)-HNE-1,N^2-dGuo adduct, the (6*S*,8*R*,11*S*)-1,N^2-dGuo lesion remained in the ring-closed conformation at the active site. The incoming dNTP, either dGTP or dATP, was positioned with Watson−Crick pairing opposite the template 5′-neighbor base, dCyt or dThy, respectively. In contrast, for the 18-mer:14-mer template-primers with a primed (6*S*,8*R*,11*S*)-HNE-1,N^2-dGuo:dCyd pair, ring opening of the adduct to the corresponding N^2-dGuo aldehyde species occurred. This allowed Watson−Crick base pairing at the (6*S*,8*R*,11*S*)-HNE-1,N^2-dGuo:dCyd pair.

INTRODUCTION

trans-4-Hydroxynonenal (HNE) is produced metabolically from membrane lipids,[1] and it is the major in vivo peroxidation product of *ω*-6 polyunsaturated fatty acids.[2,3] Several pathways for the formation of HNE from *ω*-6 polyunsaturated fatty acids have been described.[4−6] HNE exhibits a range of biological effects, from alteration of gene expression and cell signaling to cell proliferation and apoptosis.[7−13] Human exposure of HNE has been implicated in the etiologies of a number of diseases associated with oxidative stress, including Alzheimer's disease,[14] Parkinson's disease,[15] arteriosclerosis,[16] and hepatic ischemia reperfusion injury.[17] Additionally, HNE induces the SOS response in *Escherichia coli*.[18] Chromosomal aberrations are

Received: October 25, 2011
Published: February 7, 2012

observed upon exposure to HNE in rodent,[19,20] mammalian,[21,22] and human[23] cells. This suggests that HNE may be genotoxic.

Michael addition of the N^2-amino group of dGuo to HNE followed by ring closure of N1 onto the aldehyde results in four diastereomeric 1,N^2-dGuo (1,N^2-HNE-dGuo) adducts (Scheme 1),[24−27] which have been detected in cellular DNA.[28−34] The

Scheme 1. Formation of Four Diastereomeric 1,N^2-dGuo Adducts of HNE

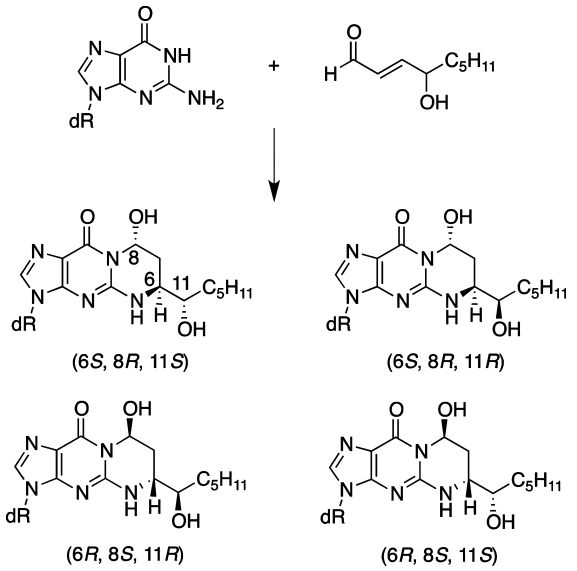

exocyclic ring of the 1,N^2-HNE-dGuo adducts blocks Watson−Crick hydrogen bonding. When placed opposite dCyd in DNA, the 1,N^2-HNE-dGuo adducts undergo ring opening to diastereomeric (6*S*,8*R*,11*S*)- and (6*R*,8*S*,11*R*)-N^2-HNE-dGuo adducts that exist primarily as minor groove cyclic hemiacetals; this ring opening exposes the Watson−Crick base-pairing face (Scheme 2).[35]

Scheme 2. (A) Formation of the Ring Open Species and (B) Watson−Crick Hydrogen Bonding of the Ring Open Hemiacetal Species with dCyd

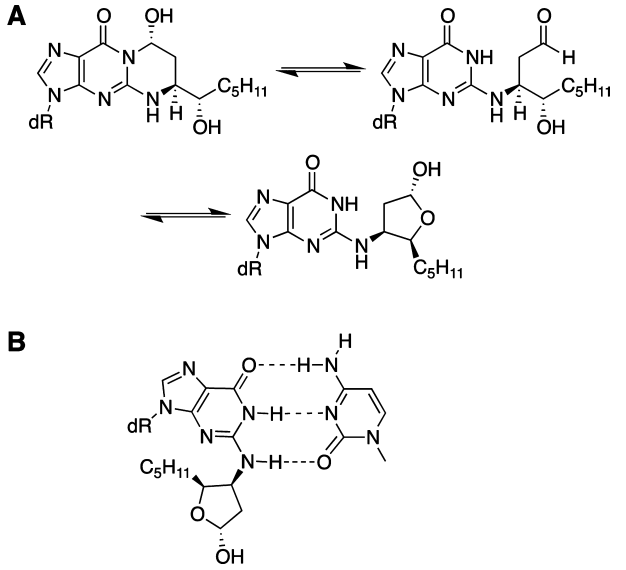

The HNE-dGuo lesions are repaired by the nucleotide excision repair pathway.[36−38] In mammalian cells, the genotoxicity of HNE depends upon glutathione levels, which modulate the formation of HNE-DNA adducts.[39−41] HNE is mutagenic and carcinogenic in rodent cells.[42,43] Hussain et al.[44] reported that HNE caused Gua → Thy transversions at codon 249 of wild-type p53 in lymphoblastoid cells. Hu et al.[45] reported that HNE-DNA adducts were preferentially formed with guanine at the third base of codon 249 in the p53 gene. The mutational spectrum induced by HNE adducts in the *supF* gene of shuttle vector pSP189 replicated in human cells showed that HNE induced primarily Gua → Thy transversions, accompanied by lower levels of Gua → Ade transitions.[36] Fernandes et al.[46] conducted site-specific mutagenesis studies and observed that the (6*S*,8*R*,11*S*)- and (6*R*,8*S*,11*R*)-1,N^2-HNE-dGuo adducts were mutagenic, inducing low levels of Gua → Thy transversions and Gua → Ade transitions. The propensity of the 1,N^2-HNE-dGuo adducts to undergo ring opening when placed opposite dCyd in DNA, potentially facilitating lesion bypass by Y-family polymerases, may account for the low levels of mutations associated with these lesions.[46]

The *Sulfolobus solfataricus* P2 DNA polymerase IV (Dpo4) is a DinB homologue that belongs to the Y-family of DNA polymerases characterized by their low fidelity on undamaged DNA templates and propensity to traverse normally replication-blocking lesions. Crystal structures of the Dpo4 polymerase in complex with unmodified DNA and the incoming nucleotide provide excellent models for investigating the structural features that determine lesion bypass efficiency and fidelity.[47−49]

To investigate the bypass of the (6*S*,8*R*,11*S*)-HNE-1,N^2-dGuo adduct by the Dpo4 polymerase, the lesion was incorporated into the 18-mer templates 5′-d-(TCATXGAATCCTTCCCCC)-3′ and 5′-d-(TCACXGAATCCTTCCCCC)-3′, for which X = (6*S*,8*R*,11*S*)-HNE-1,N^2-dGuo adduct (Chart 1).[50] These two

Chart 1. Template-Primers Utilized for Replication Bypass Studies in Vitro and Crystallography[a]

5′- GGGGGAAGGATTC -3′ 3′- CCCCCTTCCTAAGXCACT -5′	Template-Primer I
5′- GGGGGAAGGATTC -3′ 3′- CCCCCTTCCTAAGXTACT -5′	Template-Primer II
5′- GGGGGAAGGATTCC -3′ 3′- CCCCCTTCCTAAGXCACT -5′	Template-Primer III
5′- GGGGGAAGGATTCC -3′ 3′- CCCCCTTCCTAAGXTACT -5′	Template-Primer IV

[a]X = 6*S*,8*R*,11*S*-HNE-1,N^2-dGuo adduct.

templates differed in the identity of the 5′-neighbor template base, which was either Thy or Cyt, respectively. Each of these two templates was annealed either with a 13-mer primer 5′-d(GGGGGAAGGATTC)-3′ or a 14-mer primer 5′-d-(GGGGGAAGGATTCC)-3′. The 13-mer primer allowed analysis of dNTP incorporation opposite the (6*S*,8*R*,11*S*)-HNE-1,N^2-dGuo adduct, whereas the 14-mer primer allowed analysis of further extension of the (6*S*,8*R*,11*S*)-HNE-1,N^2-dGuo:dCyd template-primer terminus. This resulted in the examination of four distinct template-primer complexes

dx.doi.org/10.1021/tx200460j | *Chem. Res. Toxicol.* 2012, 25, 422−435

involving the (6*S*,8*R*,11*S*)-HNE-1,N^2-dGuo adduct (Chart 1). Replication bypass studies in vitro revealed that for both template sequences, Dpo4 had difficulty inserting dNTPs opposite the (6*S*,8*R*,11*S*)-HNE-1,N^2-dGuo adduct. However, when presented with a primed (6*S*,8*R*,11*S*)-HNE-1,N^2-dGuo:dCyd pair, the Dpo4 polymerase was in both instances able to conduct full-length extension. It was possible to obtain structures for ternary (Dpo4-DNA-dNTP) complexes with all four template-primers. The resulting structures show that when confronted with the (6*S*,8*R*,11*S*)-HNE-1,N^2-dGuo adduct at the template-primer junction in either sequence (template-primers I and II), the Dpo4 polymerase utilizes a "type II" mechanism[47] to insert either dGTP or dATP opposite the 5′-neighbor template base. In contrast, extension past a primed (6*S*,8*R*,11*S*)-HNE-1,N^2-dGuo:dCyd pair in template-primers III and IV occurs via a "type I" mechanism[47] in which the (6*S*,8*R*,11*S*)-HNE-1,N^2-dGuo adduct has undergone ring opening to the corresponding N^2-dGuo aldehyde species. The results provide a rationale for the replication bypass results in vitro.

MATERIALS AND METHODS

Materials. The Dpo4 was expressed in *E. coli* and purified using heat denaturation, Ni^{2+}-nitriloacetate chromatography, and ion-exchange chromatography as described by Zang et al.[51] All dNTPs were obtained from Amersham Biosciences (Piscataway, NJ). Unmodified oligodeoxynucleotides were synthesized and purified by Midland Certified Reagent Co. (Midland, TX), with analysis by MALDI mass spectrometry. The oligodeoxynucleotides 5′-d(TCATXGAATCCTTCCCCC)-3′ and 5′-d(TCACXGAATCCTTCCCCC)-3′ were synthesized and purified by anion-exchange chromatography by the Midland Certified Reagent Co. The 1,N^2-HNE-dGuo adduct of (6*S*,8*R*,11*S*) configuration was incorporated into both sequences [X = (6*S*,8*R*,11*S*)-1,N^2-HNE-dGuo] as reported.[50,52] The oligodeoxynucleotides were characterized by MALDI-TOF mass spectrometry. Capillary gel electrophoresis and C-18 HPLC confirmed their purities. The 18-mer template containing either a 5′-Cyt or a Thy neighbor to the (6*S*,8*R*,11*S*)-HNE-1,N^2-dGuo adduct was annealed with either the 13- and the 14-mer primers at a 1:1 molar ratio in 0.1 M NaCl, 10 mM NaH_2PO_4, and 50 μM Na_2EDTA (pH 7.2) (Chart 1), heated to 95 °C for 5 min, and then cooled to room temperature. No degradation or oxidation of the samples was observed under these conditions. The duplexes were eluted from DNA grade hydroxylapatite (Bio-Rad Laboratories, Richmond, CA) with a gradient from 10 to 200 mM NaH_2PO_4 in 10 mM NaH_2PO_4, 0.1 M NaCl, and 50 μM EDTA (pH 7.0). Duplexes were desalted with Sephadex G-25 (Sigma-Aldrich, St. Louis, MO). Oligodeoxynucleotide concentrations were determined by UV absorption at 260 nm, using calculated extinction coefficients for both sequences of 1.1×10^5 L mol^{-1} cm^{-1}.[53]

Single-Nucleotide Insertion Assays. These experiments used either a (6*S*,8*R*,11*S*)-HNE-1,N^2-dGuo adducted or nonadducted 18-mer·13-mer and 18-mer·14-mer, template·primer 5′-d(TCAYXGAATCCTTCCCCC)-3′·5′-d(GGGGGAAGGATTC)-3′ and 5′-d(TCAYXGAATCCTTCCCCC)-3′·5′-d(GGGGGAAGGATTCC)-3′, where X is either (6*S*,8*R*,11*S*)-HNE-1,N^2-dGuo adduct or Gua and Y is either Thy or Cyt, respectively (Chart 1). The ^{32}P-labeled primer was annealed to the unmodified or modified templates by heating a 1:1 molar ratio in 50 mM Tris-HCl buffer (pH 7.8) to 95 °C for 5 min and then cooling to room temperature. Primers annealed to unmodified or modified DNA templates were extended in the presence of single dNTPs. Each reaction was initiated by adding 2 μL of dNTP (final concentrations of 10, 20, and 30 μM) to a preincubated template/primer/polymerase mixture [final concentrations of 50 mM Tris-HCl (pH 7.8), 50 mM NaCl, 5 mM $MgCl_2$, 1 mM DTT, 50 μg/mL BSA, 100 nM DNA duplex, and 100 nM Dpo4] at 37 °C, yielding a reaction volume of 10 μL. The reaction mixtures for the unmodified template:primers were incubated for 15 min, and the modified template:primers were incubated for 30 min and, in both cases, 2 h for the extension in the presence of all four dNTPs. The final dNTP concentrations were 0, 10, 20, and 30 μM for incorporation of single nucleotide and extension studies. Each reaction was quenched with 50 μL of 20 mM Na_2EDTA (pH 9.0) in 95% formamide (v/v), and each mixture was heated for 10 min at 95 °C.

Full-Length Polymerase Extension Assays. For full-length extension assays, the unmodified and modified primers were extended in the presence of all four dNTPs. Each reaction was initiated by adding 2 μL of all four dNTPs (final concentrations of 10, 20, and 30 μM) to a preincubated template/primer/polymerase reaction mixture [final concentrations of 50 mM Tris-HCl (pH 7.8), 50 mM NaCl, 5 mM $MgCl_2$, 1 mM DTT, 50 μg/mL BSA, 100 nM DNA duplex, and 100 nM Dpo4] at 37 °C, yielding a reaction volume of 10 μL. The reaction mixtures for the unmodified template:primers were incubated for 15 min, and the modified template:primers were incubated for 120 min. Each reaction was quenched with 50 μL of 20 mM Na_2EDTA (pH 9.0) in 95% formamide (v/v), and each mixture was heated for 10 min at 95 °C. A denaturing gel containing 8.0 M urea and 16% acrylamide (w/v) (from a 19:1 acrylamide/bisacrylamide solution, AccuGel, National Diagnostics, Atlanta, GA) with 80 mM Tris borate buffer (pH 7.8) containing 1 mM Na_2EDTA was used for electrophoresis on which aliquots of 6 μL were separated. The gel was exposed to a PhosphorImager screen (Imaging Screen K, Bio-Rad) overnight. The bands were visualized with a PhosphorImaging system (Bio-Rad, Molecular Imager FX) using the manufacturer's software Quantity One, version 4.3.0.

Crystallization of Dpo4:DNA Complexes. The Dpo4 polymerase was concentrated to 50−70 mg/mL using a spin concentrator with a 10^4 M_r Amicon cutoff filter (Millipore, Inc., Billerica, MA) in 50 mM Tris-HCl (pH 7.4 at 25 °C) buffer containing 100 mM NaCl, 5 mM β-mercaptoethanol, and 50% glycerol (v/v). The Dpo4 polymerase was combined with template:primer DNA (1:1.2 molar ratio) and then placed on ice for 1 h prior to incubation with 1 mM d(N)TP and 5 mM $CaCl_2$. Crystals were grown using the sitting drop vapor diffusion method by mixing 1 μL of complex with 1 μL of a solution containing 50 mM Tris-HCl (pH 7.4 at 25 °C) buffer, 12−20% polyethylene glycol 3350 (w/v), 100 mM $Ca(OAc)_2$, and 2.5% glycerol (v/v). Crystals were soaked in mother liquor containing an additional 25% polyethylene glycol 3350 (w/v) and 15% ethylene glycol (v/v) and flash-frozen in a stream of liquid nitrogen.

X-ray Diffraction Data Collection and Processing. Diffraction data sets for binary and ternary complexes were collected at 110 K using a synchrotron radiation wavelength 1.0 Å on the 21-ID (Life Science Collaborative Access Team, LS-CAT) beamline at the Advanced Photon Source (Argonne, IL). Indexing and scaling were performed using HKL2000.[54] The data were processed using CCP4 package programs, and the truncate procedure was performed with TRUNCATE.[55]

Structure Determination and Refinement. The complex of the Dpo4 polymerase with the 1,N^2-εGuo lesion[51] (PDB entry: 2BQU) (a refined structure downloaded from Protein Data Bank) was used as a starting model by removing water molecules and modifying the template and primer and inserting the (6*S*,8*R*,11*S*)-HNE-1,N^2-dGuo adduct. The cross-rotation and cross-translation functions were used to align the model with the experimental data. In each instance, several rounds of rigid body refinement of the diffraction data, with gradually increasing resolution, optimized the initial positions of the models. The model was refined further using CNS Solve (version 1.1),[56] including simulated annealing, gradient minimization, individual occupancy, and refinement of individual isotropic temperature factors. Manual model building was performed using TURBO-FRODO.[57,58] A total of 5−10% of the reflections were excluded from the refinement to calculate the cross-validation residual R_{free}. Water oxygen atoms were added into positive regions (more than 3.0 standard deviations) of $F_o - F_c$ Fourier difference electron density during the manual model rebuilding steps. The crystallographic figures were prepared using PyMOL.[59]

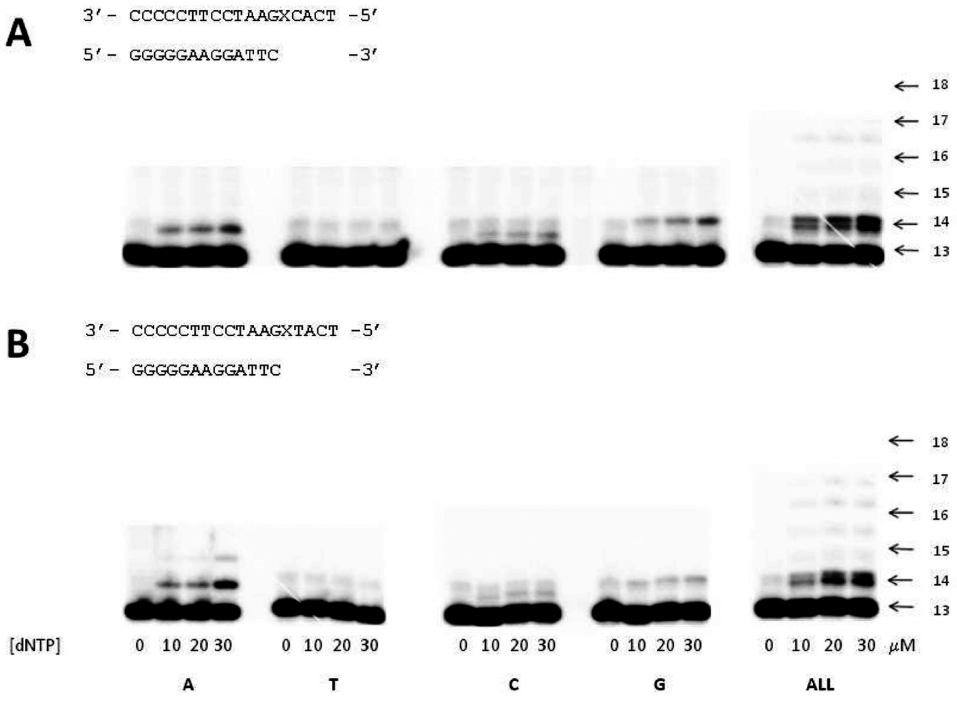

Figure 1. Replication bypass of the HNE-dGuo modified template-primer complexes I and II with *S. solfataricus* P2 DNA polymerase Dpo4. The template-primers I and II are displayed with the gels. The concentrations of the dNTPs are provided below the gels. The designations A, T, C, and G represent single-nucleotide insertion experiments; the designation ALL represents the full-length extension assay incorporating all four dNTPs. Each assay was incubated for 30 min for single-nucleotide incorporations and 2 h for extensions at 37 °C.

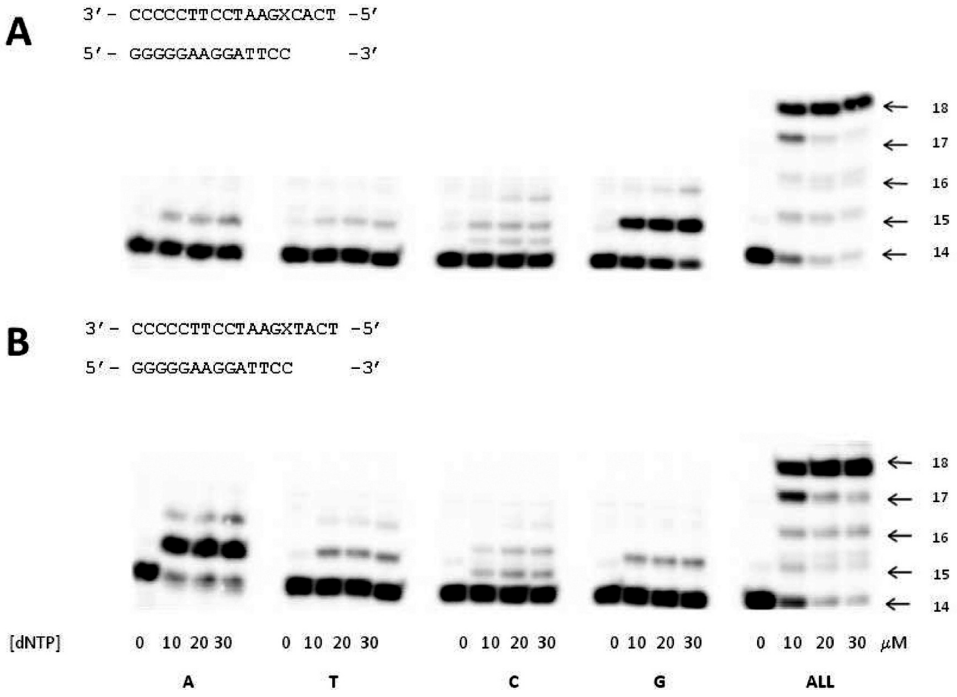

Figure 2. Extension past the HNE-dGuo modified template-primer complexes III and IV with *S. solfataricus* P2 DNA polymerase Dpo4. The template-primers III and IV are displayed with the gels. The concentrations of the dNTPs are provided below the gels. The designations A, T, C, and G represent single-nucleotide insertion experiments; the designation ALL represents the full-length extension assay incorporating all four dNTPs. Each assay was incubated for 30 min for single-nucleotide incorporations and 1 h for extensions at 37 °C.

RESULTS

Single-Nucleotide Insertion Assays. The results of single nucleotide insertion assays using the modified 18-mer:13-mer template-primers I and II (Chart 1) are shown in Figure 1. The experiments shown in Figure 1 examined the insertion of dNTPs opposite the (6*S*,8*R*,11*S*)-HNE-1,N^2-dGuo adduct in the 5′-CXG-3′ and 5′-TXG-3′ templates. Under these conditions, and using the 5′-CXG-3′ template (top panel), insertion of dNTPs after 30 min was minimal, but a preference for low levels of mis-insertion of dATP and to a lesser extent,

dx.doi.org/10.1021/tx200460j | *Chem. Res. Toxicol.* 2012, 25, 422–435

Table 2. Crystal Data and Refinement Parameters for the Ternary Dpo4-dNTP Complexes with HNE-Modified DNA[a]

parameter	5′-CXG-3′	5′-TXG-3′	5′-CXG-3′	5′-TXG-3′
beamline	LS-CAT (ID-D)	LS-CAT (ID-G)	LS-CAT (ID-D)	LS-CAT (ID-G)
sequence	I	II	III	IV
wavelength (Å)	1.08	0.978	1.08	0.978
temperature (K)	100	100	100	100
space group	$P2_12_12$	$P2_12_12$	$P2_12_12$	$P2_12_12$
unit cell (a, b, c; Å)	94.82, 102.86, 53.15	95.01, 103.06, 53.22	95.12, 103.72, 53.82	94.37, 104.01, 52.83
resolution range (Å)	30−2.35	30−2.4	30−2.6	30−2.9
highest resolution shell	2.39−2.35	2.44−2.4	2.64−2.6	2.95−2.9
no. of measurements	144724	149646	115578	84922
no. of unique reflections	22417 (1117)	21023 (1010)	16566 (841)	12102 (601)
redundancy	7.4 (6.5)	7.1 (6.0)	7.0 (6.6)	7.0 (6.2)
completeness (%)	99.6 (100.0)	99.8 (98.1)	99.6 (100.0)	99.9 (100.0)
R_{merge} (%)[b]	4.9 (23.3)	5.5 (40.7)	7.0 (34.7)	8.0 (43.0)
signal to noise ($I/\sigma I$)	39.4 (6.6)	37.3 (3.1)	32.3 (4.0)	25.6 (2.8)
solvent content (%)	56.38	56.62	56.61	56.41
model composition (asymmetric unit)				
no. amino acid residues	342	342	342	342
no. water molecules	181	131	111	91
no. of Ca^{2+} ions	3	3	3	3
no. template nucleotides	17	17	17	17
no. primer nucleotides	13	13	14	14
no. dATPs		1		1
no. dGTPs	1		1	
R_f (%)[c]	21.7	22.1	20.5	21.5
R_{free} (%)[d]	25.7	24.9	26.7	26.3
estimated coordinate error (Å)				
from Luzatti plot	0.31	0.34	0.35	0.37
from Luzatti plot (c-v)	0.37	0.44	0.49	0.50
from σA plot	0.28	0.35	0.29	0.33
from σA plot (c-v)	0.35	0.43	0.39	0.47
temperature factors				
Wilson plot (Å^2)	50.1	53.5	35.0	42.4
mean isotropic (Å^2)	47.6	50.7	48.2	54.5
rmsd in temperature factors				
bonded main chain atoms (Å^2)	1.49	1.55	1.41	1.44
bonded side chain atoms (Å^2)	2.34	2.32	2.20	2.19
rmsd from ideal values				
bond lengths (Å)	0.007	0.007	0.007	0.008
bond angles (°)	1.3	1.4	1.4	1.4
dihedral angles (°)	20.9	21.2	20.9	21.3
improper angles (°)	1.2	1.2	1.2	1.2

[a] rmsd, root mean square deviation; and c-v, cross-validation. Values in parentheses correspond to the highest resolution shells. [b] $R_{merge} = \Sigma_{hkl} \Sigma_{j=1,N} |\langle I_{hkl} \rangle - I_{hklj}| / \Sigma_{hkl} \Sigma_{j=1,N} |I_{hklj}|$, where the outer sum ($hkl$) is taken over the unique reflections. [c] $R_f = \Sigma_{hkl} ||F_{o,hkl}| - k|F_{c,hkl}|| / \Sigma_{hkl} |F_{o,hkl}|$, where $|F_{o,hkl}|$ and $|F_{c,hkl}|$ are the observed and calculated structure factor amplitudes, respectively. [d] R_{free} is same as for R_f for the set of reflections (5−10% of the total) omitted from the refinement process.

dGTP, were observed. Interestingly, two bands were observed when all dNTPs were included in the reaction. Presumably, the addition of dATP or dGTP gave products that migrated to different positions in the gel. When all dNTPs were included in the reaction, the Dpo4 polymerase failed to extend the primer to the full length after 2 h (Figure 1). The bottom panel shows the results of single-nucleotide insertion assays using the 18-mer:13-mer template-primer II, containing the 5′-TXG-3′ sequence (Chart 1). These experiments were also conducted for 30 min in the case of incorporation of single nucleotides and 2 h for the extension. Again, the polymerase exhibited low levels of error-prone incorporation of dATP and to a lesser extent, dGTP, opposite to the adduct. Again, two bands were observed when all dNTPs were included in the reaction. Presumably, the addition of dATP or dGTP gave products that migrated to different positions in the gel. When all dNTPs were included in the reaction, the polymerase failed to extend the primer to full length.

The results of single-nucleotide extension assays using the modified 18-mer:14-mer template-primers III and IV (Chart 1) are shown in Figure 2. The corresponding single-nucleotide insertion assays using the unmodified template-primers are shown in Figure S1 in the Supporting Information. The experiments shown in Figure 2 examined the extension of dNTPs beyond a primed (6*S*,8*R*,11*S*)-HNE-1,N^2-dGuo:dCyd pair in the 5′-CXG-3′ and 5′-TXG-3′ templates. The Dpo4 polymerase exhibited primarily an error-free incorporation of dGTP with the 5′-CXG-3′ template. When all dNTPs were

dx.doi.org/10.1021/tx200460j | *Chem. Res. Toxicol.* 2012, 25, 422−435

included in the reaction, the polymerase efficiently extended the primer to the full-length 18-mer product. Primarily error-free incorporation of dATP was observed for the 5′-TXG-3′ template (template-primer IV); efficient extension to a full-length 18-mer product was also observed when all dNTPs were included in the reaction. In all instances, these experiments were conducted for 30 min in case of incorporation of single nucleotides and 1 h for the extension.

Crystallization, Data Collection, and Data Processing. Crystallization trials were conducted with each of the (6*S*,8*R*,11*S*)-HNE-1,N^2-dGuo modified 18-mer templates-primer complexes (I–IV, Chart 1), Dpo4, each of the four dNTPs, and Ca^{2+}. The Dpo4 polymerase shows weak activity in the presence of Ca^{2+}.[60,61] A concentration range of 7–15 mg/mL of the Dpo4 polymerase was used to find the optimum concentration for growing crystals that diffracted well. The Dpo4 polymerase cocrystallized with the 5′-CXG-3′ template-primers I and III in the presence of dGTP and with the 5′-TXG-3′ template-primers II and IV in the presence of dATP. All of the complexes crystallized in the orthorhombic crystal system in the space group $P2_12_12$. (The data were of good overall completeness and showed sufficient redundancy.) These crystals diffracted between 2.35 and 2.9 Å. The statistics of data processing and data quality for these ternary complexes are summarized in Table 2.

Formation of "Type II" Complexes When the (6*S*,8*R*,11*S*)-HNE-1,N^2-dGuo Was Positioned at the Template-Primer Junction (Template-Primers I and II). The structure of the ternary Dpo4-DNA-dGTP complex with 5′-CXG-3′ template paired with a −1 primer (I) was determined at 2.35 Å resolution. Figure 3 depicts the catalytic core shown with electron density for the adducted and neighboring region. The Dpo4 polymerase active site resembled the "type II" structure with native DNA.[47] The active site accommodated the (6*S*,8*R*,11*S*)-HNE-1,N^2-dGuo adduct and its 5′-template dCyd neighbor. The (6*S*,8*R*,11*S*)-HNE-1,N^2-dGuo adduct remained ring-closed. The incoming dGTP was positioned to form Watson–Crick hydrogen bonds with the 5′-template dCyd neighbor. The 1,N^2-dGuo exocyclic ring was inserted into the duplex such that the incoming dGTP could not orient in the Watson–Crick plane. This resulted in a gap of 7.5 Å between the 3′-hydroxyl of the primer dCyd and the α-phosphate of the incoming dGTP. This was unlikely to represent a catalytically competent conformation. Three bound Ca^{2+} ions were identified. The first two were in the active site and involved with dGTP coordination. The third was 3.0 Å from the main chain carbonyl oxygen of Ala181 in the thumb domain of the polymerase. Arg336 was bent toward the template DNA backbone and formed a hydrogen bond with the phosphate oxygen. The alkyl chain of the (6*S*,8*R*,11*S*)-HNE-1,N^2-dGuo adduct was partly visible in Figure 3A,C and was presumably oriented toward the minor groove. The three 5′-terminal template nucleosides exhibited electron density for the deoxyribose sugars and partial density for the nucleobases with thermal parameters of 100–120, which suggested that they were partially disordered.

The structure of the ternary Dpo4-DNA-dATP complex with 5′-TXG-3′ template paired with a −1 primer (II) was determined at 2.4 Å resolution. The catalytic core is shown with electron density for the adducted and neighboring region (Figure 4). Again, the polymerase active site resembled the "type II" structure with native DNA.[47] It accommodated the (6*S*,8*R*,11*S*)-HNE-1,N^2-dGuo adduct and its 5′-template dThd

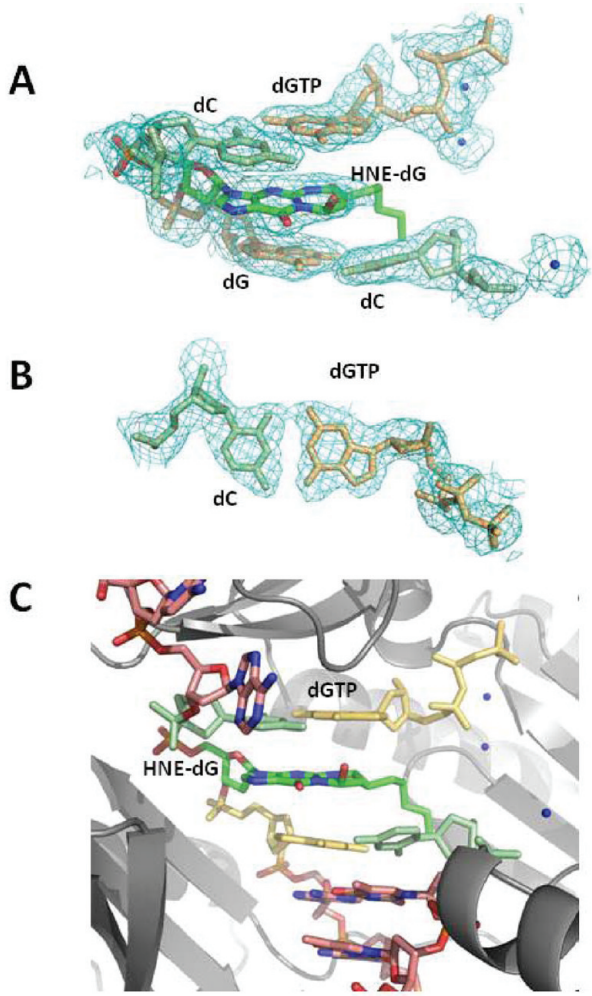

Figure 3. Structure of the ternary HNE-dGuo-modified template-primer I complex with the *S. solfataricus* P2 DNA polymerase Dpo4 and incoming dGTP. (A) Electron density at the active site. (B) Watson–Crick base pair between the 5′-template neighbor C and incoming dGTP. (C) Active site with the modified template-primer and the dGTP along with the polymerase. The Dpo4 is colored gray and shown in cartoon form. All electron densities are from $(2F_o - F_c)$ maps at the 1σ level. The HNE alkyl chain is disordered, resulting in some uncertainty in its position.

neighbor. The 1,N^2-dGuo exocyclic ring was inserted into the duplex such that the incoming dATP could not orient in the Watson–Crick plane. The 5′-dThd was positioned to form Watson–Crick hydrogen bonds with the incoming dATP, which resulted in a gap of 7.4 Å between the 3′-hydroxyl of the primer dCyd and the α-phosphate of the dATP. This is unlikely to represent a catalytically competent conformation. Of three bound Ca^{2+} ions, one was at the active site and 3.5 Å distant from the 3′-terminal hydroxyl of the primer, suggesting that it was positioned to catalyze the reaction. Again, the electron density for the alkyl side chain of the (6*S*,8*R*,11*S*)-HNE-1,N^2-dGuo adduct was weak, but the side chain was presumably directed into minor groove. The 5′-end of the template was also disordered, and three bases on that side of the adduct were seen with higher thermal parameters.

Extension Beyond a Primed (6*S*,8*R*,11*S*)-HNE-1,N^2-dGuo:dCyd Base Pair (Template-Primers III and IV). The structure of the ternary Dpo4-DNA-dGTP complex involving the 5′-CXG-3′ template in which the (6*S*,8*R*,11*S*)-

dx.doi.org/10.1021/tx200460j | *Chem. Res. Toxicol.* 2012, 25, 422–435

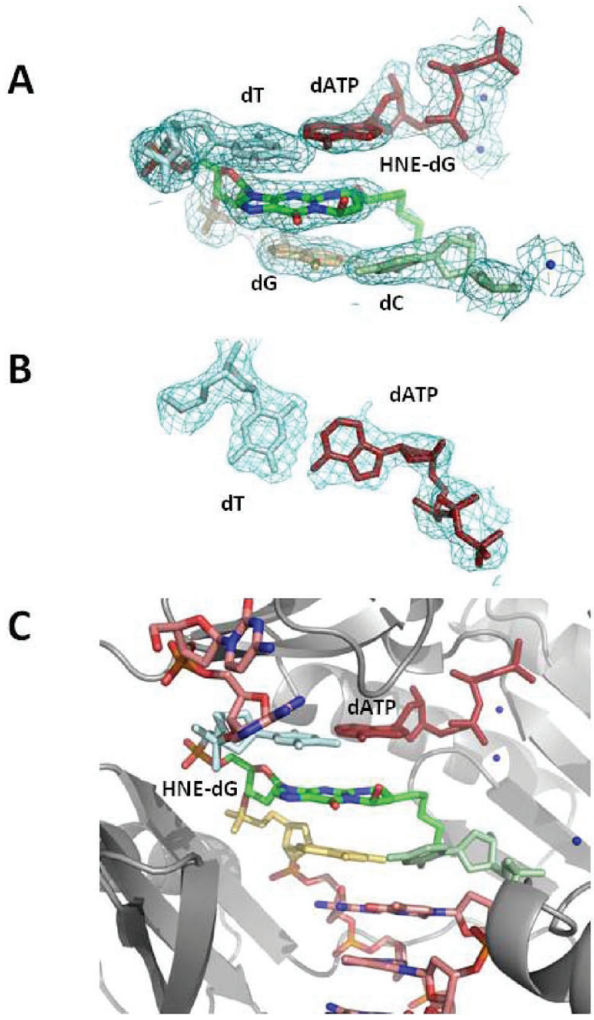

Figure 4. Structure of the ternary HNE-dGuo modified template-primer II complex with the *S. solfataricus* P2 DNA polymerase Dpo4 and incoming dATP. (A) Electron density at the active site. (B) Watson−Crick base pair between the 5′-template neighbor T and incoming dATP. (C) Active site with the modified template:primer and the dATP along with the polymerase. The Dpo4 polymerase is colored gray and shown in cartoon form. All electron densities are from $(2F_o - F_c)$ maps at the 1σ level. The HNE alkyl chain is disordered, resulting in some uncertainty in its position.

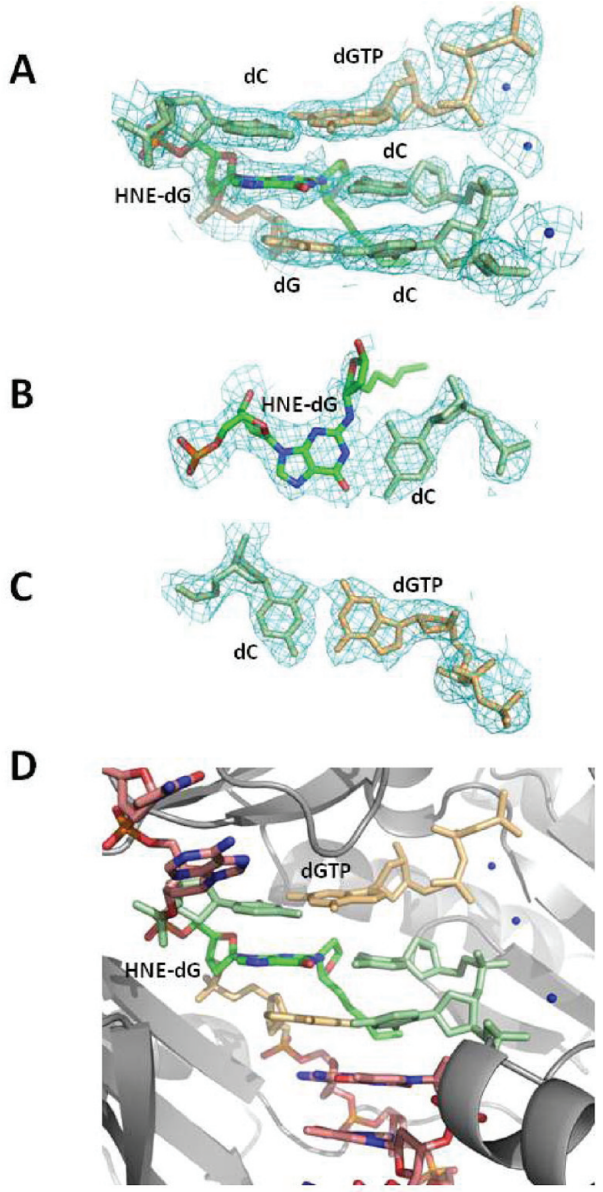

Figure 5. Structure of the ternary HNE-dGuo-modified template-primer III complex with the *S. solfataricus* P2 DNA polymerase Dpo4 and incoming dGTP. (A) Electron density at the active site. (B) Watson−Crick base pair between HNE-dGuo and 3′-primer terminus dCyd. (C) Watson−Crick base pair between the 5′-template neighbor C and the incoming dGTP. (D) Active site with the modified template:primer and the dGTP along with the polymerase. The Dpo4 polymerase is colored gray and shown in cartoon form. All electron densities are from $(2F_o - F_c)$ maps at the 1σ level.

HNE-1,N^2-dGuo adduct is paired with dCyd (III) was determined at 2.6 Å resolution. The catalytic core is shown with electron density for the adducted and neighboring region (Figure 5). The $F_o - F_c$ omit map calculated at 2σ is provided in Figure S2 in the Supporting Information. The (6*S*,8*R*,11*S*)-HNE-1,N^2-dGuo adduct underwent ring opening when paired to a complementary dCyd at the 3′ terminus of the primer (Scheme 2B). This exposed the Watson−Crick face of the damaged dGuo, allowing Watson−Crick hydrogen bonding with dCyd at the primer terminus. In this case, the incoming dGTP was positioned to form Watson−Crick hydrogen bonding with the 5′-template dCyd. The distance between the primer 3′-OH and the incoming α-phosphate of the dGTP was 5.1 Å. Huang et al.[35] used NMR spectroscopy to conclude that these aldehydic rearrangement products exist in equilibrium with stereoisomeric cyclic hemiacetals. The latter were the predominant species present at equilibrium. For the ternary Dpo4-DNA-dGTP complex involving template-primer III, it was not possible to unequivocally interpret the electron density for the HNE moiety, which may reflect this equilibrium between the aldehydic and cyclic hemiacetal forms of the adduct. To avoid model bias, the map was calculated using a simulated annealing omit map at the adduct and its complementary base sites. The electron density in Figure 5 was fitted using the cyclic hemiacetal form of the HNE moiety, which would be consistent with the NMR data.[35] Clear electron density was visible in the $F_o - F_c$ map at the 3σ level. The resulting structure predicted that the hydroxyl moiety of the cyclic hemiacetal group was within hydrogen-bonding distance of Lys78 of the finger domain of the polymerase. Tyr12 of the

dx.doi.org/10.1021/tx200460j | *Chem. Res. Toxicol.* 2012, 25, 422−435

finger domain exhibited parallel stacking with the deoxyribose of the incoming dNTP. The primer DNA backbone phosphate of the dCyd complementary to the adduct was close to a Ca^{2+} ion, with the distance to the phosphate oxygen being 3 Å. This indicated a productive complex catalyzed by the Ca^{2+} ion.

The structure with incoming dATP for the ternary complex with the 5′-TXG-3′ template in which the adduct was paired with dCyd (IV) was determined at 2.9 Å resolution (Table 2). The catalytic core is shown with the electron density map for the adducted and neighboring region (Figure 6). The $F_o - F_c$ omit map calculated at 2σ is provided in Figure S3 in the Supporting Information. In this case, the HNE moiety also underwent rearrangement to a ring open conformation. The ring-opening exposed the Watson–Crick face of the adducted base toward the dCyd of the primer (Scheme 2B). Watson–Crick hydrogen bonding was conserved for both neighboring base pairs (Figure 6C). The distance between the primer 3-OH and the incoming α- phosphate of the dATP was 5.3 Å. The Ca^{2+} binding sites were similar to the corresponding structure of template-primer complex III with incoming dGTP.

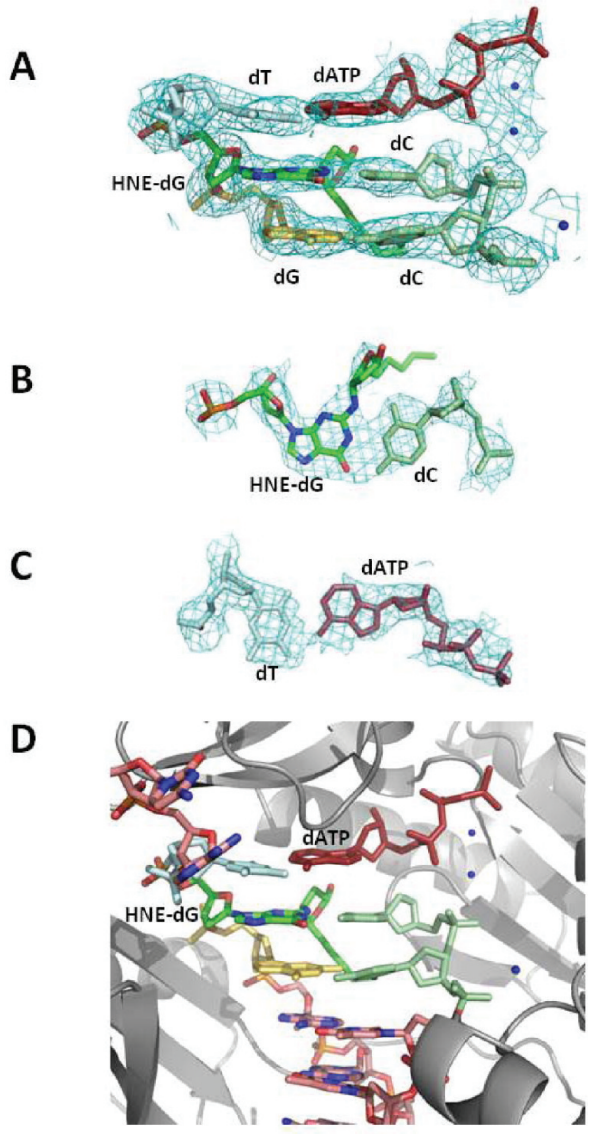

Figure 6. Structure of the ternary HNE-dGuo-modified template-primer IV complex with the *S. solfataricus* P2 DNA polymerase Dpo4 and incoming dATP. (A) Electron density at the active site. (B) Watson–Crick base pair between HNE-dGuo and 3′-primer terminus dCyd. (C) Watson–Crick base pair between the 5′-template neighbor T and the incoming dATP. (D) Active site with the modified template:primer and the dATP along with the polymerase. The Dpo4 polymerase is colored gray and shown in cartoon form. All electron densities are from $(2F_o - F_c)$ maps at the 1σ level.

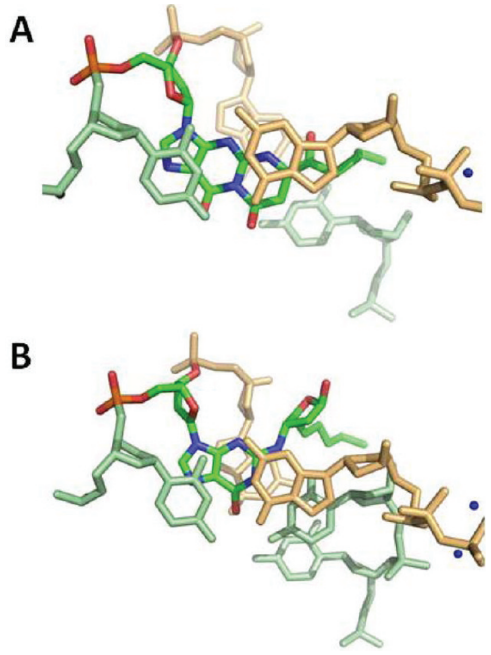

Figure 7. Stacking pattern of DNA base pair at the active site and its neighboring bases of the ternary complexes. (A) Template-primer I. (B) Template-primer III. The HNE site colors are as follows: C, green; N, blue; O, red; and P, yellow. The Ca^{2+} ions are shown as blue spheres. dCyd is green, dGuo and dGTP are gold.

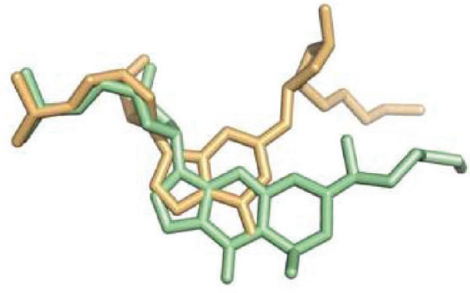

Figure 8. Overlay of the ring close (green) and ring open (gold) HNE-dGuo moieties along with the sugar and phosphate backbone for template-primer complexes I and III.

DISCUSSION

The observations that HNE induces the SOS response in *E. coli*[18] and that chromosomal aberrations are observed upon exposures to HNE in rodent,[19,20] mammalian,[21,22] and human[23] cells implicate it as a genotoxic species. In fact, HNE is mutagenic and carcinogenic in rodent cells.[42,43] Hussain et al.[44] have reported that HNE causes Gua → Thy transversions at codon 249 of wild-type p53 in lymphoblastoid cells. The mutation spectrum induced by HNE adducts in the *supF* gene

dx.doi.org/10.1021/tx200460j | *Chem. Res. Toxicol.* 2012, 25, 422–435

of shuttle vector pSP189 replicated in human cells shows that it induces primarily Gua → Thy transversions, accompanied by lower levels of Gua → Ade transitions.[36] Hu et al.[45] have reported that HNE-DNA adducts are preferentially formed with guanine at the third base of codon 249 in the p53 gene. The synthesis of HNE-DNA adducts[50] enabled site-specific mutagenesis studies. Fernandes et al.[46] have observed that the (6*S*,8*R*,11*S*)- and (6*R*,8*S*,11*R*)-1,N^2-HNE-dGuo adducts induce low levels of Gua → Thy transversions and Gua → Ade transitions. The propensity of the 1,N^2-HNE-dGuo adducts to undergo ring opening when placed opposite dCyd in DNA,[35] potentially facilitating lesion bypass by Y-family polymerases, may account for the low levels of mutations associated with these lesions. The Dpo4 polymerase is a DinB homologue that belongs to the Y-family of DNA polymerases.[47,62,63] Structures of the Dpo4 polymerase in complex with modified DNA and incoming dNTPs provide models for investigating the structural features that determine lesion bypass efficiency and fidelity.[47]

Replication Bypass of the (6*S*,8*R*,11*S*)-HNE-1,N^2-dGuo Adduct. The single-nucleotide insertion assays using either the template-primer I or II (Figure 1) indicate that the Dpo4 polymerase preferentially inserts purine dNTPs opposite to the (6*S*,8*R*,11*S*)-1,N^2-dGuo adduct in a sequence-specific manner. The efficiency for correct dCTP insertion opposite the (6*S*,8*R*,11*S*)-1,N^2-dGuo adduct is low. The data suggest that for the 5′-C<u>X</u>G-3′ template, dGTP or dATP are mis-inserted opposite the lesion at similar levels. Mis-insertion of dATP is more efficient for the 5′-T<u>X</u>G-3′ template. This sequence effect would be consistent with the ability of the Y-family polymerase to utilize a "type II" insertion mechanism,[47] in which the incoming dGTP and dATP template from the 5′-neighbor dCyd and dThd, respectively. Subsequent strand realignment would lead to Gua → Cyt and Gua → Thy transversions, respectively. If strand slippage did not occur after dNTP insertion opposite the template 5′-neighbor base, then a −1 deletion would result. In any event, the multiple nucleotide insertion assays using either the template-primer I or II show that the (6*S*,8*R*,11*S*)-1,N^2-dGuo adduct hinders subsequent strand extension (Figure 1). However, extension by the Dpo4 polymerase from a primed (6*S*,8*R*,11*S*)-1,N^2-dGuo:dCyd pair in template-primers III or IV is efficient and extends to produce full-length primer (Figure 2). In this case, the strong sequence preference to insert dGTP in the template:primer III or dATP in the template:primer IV sequences is evident.

Structure−Activity Relationships. The structural analysis of the ternary complexes involving the (6*S*,8*R*,11*S*)-HNE-1,N^2-dGuo adduct at the template-primer junction (I and II) suggests that the exocyclic ring of adduct sterically hinders incoming dNTPs from achieving the proper geometry within the active site of the Dpo4 polymerase. The electron density at the active site indicates that the alkyl chain is in the minor groove (Figure 3). This provides a rationale for the inefficient bypass of the (6*S*,8*R*,11*S*)-HNE-1,N^2-dGuo adduct by the polymerase (Figure 1). The ternary complexes of template-primers I and II with the (6*S*,8*R*,11*S*)-HNE-1,N^2-dGuo modified templates with the Dpo4 polymerase resemble "type II" complexes,[47] in which the incoming correct dNTPs skip the (6*S*,8*R*,11*S*)-HNE-1,N^2-dGuo base and form Watson−Crick hydrogen bonds with the 5′- neighboring template nucleotides, either dCyd or dThd. These "type II" complexes result in 7.5 or 7.4 Å distances between the 3′-hydroxyl of the primers and the α-phosphates of the incoming dNTPs, for the template-primers I and II, respectively. Overall, the structures of the DNA and protein for the complexes involving template-primers I and II are comparable with a root-mean-square deviation (rmsd) of 0.4 Å for the backbone atoms. In both instances, the template backbone is stretched to fit the DNA into the catalytic core of the polymerase. These structures are unlikely to represent catalytically competent conformations since the distances between the 3′-hydroxyls of the primer and the α-phosphates of the incoming dNTPs are 7.5 and 7.4 Å, respectively. This is consistent with the low efficiency for dGTP and dATP insertions opposite the (6*S*,8*R*,11*S*)-HNE-1,N^2-dGuo adduct in the 5′-C<u>X</u>G-3′ and 5′-T<u>X</u>G-3′ templates, respectively (Figure 1). It is unclear what structural changes need to occur to bring these atoms close enough so that the reaction could occur.

The structural analysis of the ternary complexes in which a dCyd was positioned opposite the lesion (template-primers III and IV) illustrates how exocyclic ring opening to a N^2-HNE-dGuo:dCyd base pair can promote Watson−Crick pairing. These two structures provide the first evidence that the ring-opened form of the (6*S*,8*R*,11*S*)-HNE-1,N^2-dGuo adduct is accommodated within the Y-family polymerase active site. Structures with the Dpo4 polymerase and the malondialdehyde-induced 3-(2′-deoxy-β-D-*erythro*-pentofuranosyl)-pyrimido[1,2-α]purin-10(3*H*)-one (M_1dGuo) adduct showed only the ring-closed form of that lesion in the active site,[64] as did structures of the 1,N^2-propano-dGuo (PdGuo) adduct,[65] which cannot undergo ring opening. It has been suggested that ring opening of the (6*S*,8*R*,11*S*)-HNE-1,N^2-dGuo facilitates lesion bypass by Y-family polymerases, which may account for the low levels of mutations associated with these lesions.[46] The single-nucleotide insertion assays with the 5′-C<u>X</u>G-3′ template-primer III suggest that following insertion of dCTP opposite the (6*S*,8*R*,11*S*)-HNE-1,N^2-dGuo adduct, the polymerase can insert dGTP opposite the template 5′-neighbor dCyd (Figure 2). In the case of 5′-T<u>X</u>G-3′ template-primer IV following insertion of dCTP opposite the (6*S*,8*R*,11*S*)-HNE-1,N^2-dGuo adduct, the polymerase can insert dATP opposite the template 5′-neighbor dThd (Figure 2). The ternary complex of the ring-opened N^2-HNE-dGuo:dCyd template-primer III shows insertion of dGTP opposite the 5′-template neighbor dCyd (Figure 5). The ternary complex of the adduct in template-primer IV shows insertion of dATP opposite the 5′-template neighbor dThd (Figure 6). In each instance, the incoming dNTP is properly stacked and hydrogen bonded to the 5′-template neighbor. In both the template-primers III and IV, the primed ring-opened N^2-HNE-dGuo:dCyd base pair conserves Watson−Crick hydrogen bonds, positioning the primer 3′-OH for a catalytic cycle. Both of these structures are likely to be catalytically competent, because of the 5.1 or 5.3 Å distances of the α-phosphates of the incoming dGTP or dATP and the 3′-OH groups of the primers. The second Ca^{2+} ion is in each instance positioned to play a crucial role in catalyzing the reaction.

These data provide structural evidence that ring opening of the (6*S*,8*R*,11*S*)-1,N^2-dGuo adduct facilitates extension by the Dpo4 polymerase past the lesion. Riggins et al.[66,67] reported mechanistic studies of the ring opening and closing of the related M_1dGuo. They concluded that ring opening of M_1dGuo as a nucleoside or in oligodeoxynucleotides occurred via a reversible second-order reaction with hydroxide ion and was catalyzed by the complementary cytosine in duplex DNA. The closure of the resulting N^2-(3-oxo-1-propenyl)-dGuo anion was pH-dependent, and under neutral and acidic conditions, ring

closure was biphasic, leading to the rapid formation of intermediates that slowly converted to M_1dGuo in a general acid-catalyzed reaction.

Site-specific mutagenesis in the COS-7 cell system[46] revealed that the (6*S*,8*R*,11*S*)-1,N^2-HNE-dGuo adduct was mutagenic, inducing low levels of Gua → Thy transversions and Gua → Ade transitions. The replication bypass studies, in vitro, indicate that for both template-primers I and II, the Dpo4 polymerase inserts low levels of dATP opposite the (6*S*,8*R*,11*S*)-1,N^2-HNE-dGuo adduct (Figure 1). The Dpo4 polymerase recapitulates one aspect of the site-specific mutagenesis experiments in COS-7 cells, the insertion of low levels of dATP opposite the (6*S*,8*R*,11*S*)-1,N^2-HNE-dGuo adduct, which would ultimately lead to Gua → Thy transversions. On the other hand, little to no insertion of dTTP by the Dpo4 polymerase, which would lead to Gua → Ade transitions, is observed (Figure 1). The structural studies confirm the ability of the Dpo4 polymerase to form "type II" complexes,[47] which utilize the 5′-neighboring dThd to insert dATP in the 5′-TXG-3′ template, or the 5′-neighboring dCyd to insert dGTP in the 5′-CXG-3′ template, when bypassing the (6*S*,8*R*,11*S*)-1,N^2-HNE-dGuo adduct. Further extension from "type II" complexes would result in −1 frameshifts, but if such complexes instead relaxed to form (6*S*,8*R*,11*S*)-1,N^2-HNE-dGuo:dAdo or (6*S*,8*R*,11*S*)-1,N^2-HNE-dGuo:dGuo mispairs, a second incorporation of dATP opposite the 5′-template neighbor dThd or of dGTP opposite the 5′-template neighbor dCyd would result in Gua → Thy or Gua → Cyt transversions, respectively. However, the Gua → Thy mutations observed in the site-specific mutagenesis studies using the COS-7 system involved the template 5′-C<u>X</u>A-3′ sequence,[46] which is not consistent with the generation of Gua → Thy mutations via the primate equivalent of the "type II" mechanism.

DeCarlo et al.[68] asked how purine−purine mispairs might be formed and extended by the Dpo4 polymerase, which may be relevant with respect to the preferential incorporation of purines dATP and dGTP at (6*S*,8*R*,11*S*)-1,N^2-HNE-dGuo lesions (Figure 1). They suggested that during mispair formation the newly forming base pair might be in a Hoogsteen geometry with the incoming dNTP in the anti conformation and the template base in the syn conformation. The present structural studies involving the Dpo4 polymerase do not directly address this question because all of the complexes examined herein show the template base, either the ring-closed (6*S*,8*R*,11*S*)-1,N^2-HNE-dGuo adduct or its ring-opened rearrangement product, in the anti conformation about the glycosyl bond. However, the PdGuo adduct,[69] which cannot undergo ring opening, reorients into the syn conformation in DNA. Significantly, when mispaired with dAdo, PdGuo exhibited X (*syn*)·A(*anti*) pairing at pH 5.8 and simultaneous partial intercalation of the complementary X and A bases at pH 8.9. When mispaired with dGuo, PdGuo exhibited X(*syn*)·G(*anti*) pairing, which was pH-independent.[70−73] When placed in 5′-d(CGCXCGGCATG)-3′ at pH 5.8, PdGuo induced a localized structural perturbation involving the modified base pair and its 3′-neighbor. PdGuo rotated into the *syn* conformation about the glycosyl bond, and the 3′-neighbor base pair existed in a mixture of Watson−Crick and Hoogsteen conformations.[74] In the 5′-d(CGCGGTXTCCGCG)3′·5′-d(CGCGGACACCGCG)-3′ duplex, PdGuo introduced a localized perturbation, which was pH-dependent.[75] At pH 5.2, PdGuo rotated into the *syn* conformation about the glycosyl bond, placing the exocyclic moiety into the major groove. PdGuo formed a protonated Hoogsteen pair with cytosine in the complementary strand. In this sequence, the 3′-neighbor base pair did not equilibrate between Hoogsteen and Watson−Crick base pairing.[75]

Consequently, the mechanism(s) by which COS-7 cellular bypass polymerases induce low levels of Gua → Thy transversions and Gua → Ade transitions when confronted by the (6*S*,8*R*,11*S*)-1,N^2-HNE-dGuo adduct remain to be determined. Structural investigation of ternary complexes of the (6*S*,8*R*,11*S*)-1,N^2-HNE-dGuo adduct with mammalian Y-family polymerases will thus be of considerable interest. The lesion bypass ability, accuracy, and efficiency of these polymerases vary and depend on the type of DNA lesion.[76−87] For example, the mammalian Y-family pol ι has been observed to incorporate dNTPs via Hoogsteen base pair formation.[88−90] Thus, error-free replication past the (6*S*,8*R*,11*S*)-1,N^2-HNE-dGuo adduct has been shown to be mediated by the sequential action of hPol ι and hPol κ, with hPol ι incorporating the correct dNTP opposite the lesion and hPol κ subsequently extending the primer.[91] Similar observations have been made for the structurally related γ-hydroxy-1,N^2-propanodeoxyguanosine adduct.[86]

Comparison with Structurally Related 1,N^2-dGuo Adducts. The results presented here extend our knowledge as to how the Dpo4 polymerase interacts with DNA adducts possessing 1,N^2-dGuo exocyclic rings. In all cases examined to date, the Dpo4 polymerase prefers inserting purine dNTPs opposite these lesions, particularly dATP. Replication bypass experiments showed that the Dpo4 polymerase inserted dGTP and dATP when challenged by the PdGuo adduct. The structures of ternary polymerase-DNA-dNTP complexes for three template-primer DNA sequences were determined. All three were of the "type II" structure described for ternary complexes with native DNA.[47] The PdGuo adduct remained in the anti conformation about the glycosyl bond in each of these three ternary complexes. Malondialdehyde reacts with dGuo in DNA to give the M_1dGuo adduct. The level of steady-state incorporation of dNTPs by the Dpo4 polymerase opposite M_1dGuo was reduced, but it also exhibited a preference for dATP incorporation.[64] A spectrum of products was observed during replication bypass arising principally by incorporation of dCTP or dATP opposite M_1dGuo followed by partial or full-length extension. A greater proportion of −1 deletions were observed when dThd was positioned 5′ of M_1dGuo in the template.[64] A "type II" frameshift deletion complex[47] and another complex with Dpo4 bound to a M_1dGuo:dCyd pair located in the postinsertion context. M_1dGuo was in the ring-closed state in both structures, and in the structure with dCyd opposite M_1dGuo, the dCyd nucleotide moved out of the Dpo4 active site into the minor groove.[64] The 1,N^2-etheno-dGuo is a two-carbon, as opposed to a three-carbon, annelation product of dGuo, but again, the Dpo4 polymerase preferentially incorporated dATP opposite this adduct in the 5′-TX-3′ sequence.[51] With the template 5′-CX-3′ sequence, both dGTP and dATP were incorporated. These results were consistent with the "type II" intermediate, in which the identity of the dNTP inserted opposite the lesion depends upon the 5′-neighbor template base. Additional minor extension products were observed in mass spectrometric analyses, leading to the conclusion that the Dpo4 polymerase uses several mechanisms, including dATP incorporation opposite 1,N^2-εdGuo lesions and also a variation of dNTP-stabilized misalignment, to generate both base pair and frameshift mutations.[51]

dx.doi.org/10.1021/tx200460j | *Chem. Res. Toxicol.* 2012, 25, 422−435

Summary. The Dpo4 polymerase does not efficiently insert nucleotides opposite to the (6*S*,8*R*,11*S*)-1,N^2-dGuo adduct, consistent with the low levels of Gua → Thy mutations. However, it extends past the (6*S*,8*R*,11*S*)-1,N^2-dGuo:dCyd pair. A series of ternary (Dpo4-DNA-dNTP) structures with (6*S*,8*R*,11*S*)-1,N^2-dGuo-adducted templates suggest that during replication, the ring-closed (6*S*,8*R*,11*S*)-1,N^2-dGuo lesion at the active site hinders incorporation of dNTPs opposite the lesion, whereas the ring-opened form of the lesion in the (6*S*,8*R*,11*S*)-1,N^2-dGuo:dCyd pair allows for extension to full-length product.

■ ASSOCIATED CONTENT

Ⓢ Supporting Information

Extension past the unmodified template-primer complexes III and IV with *S. solfataricus* P2 DNA polymerase Dpo4 (Figure S1); structure of the ternary HNE-dGuo-modified template-primer III complex with the *S. solfataricus* P2 DNA polymerase Dpo4 and incoming dGTP, with electron density at the adduct site calculated using omit map ($F_o - F_c$) contoured at 2σ (Figure S2); and structure of the ternary HNE-dGuo-modified template-primer IV complex with the *S. solfataricus* P2 DNA polymerase Dpo4 and incoming dATP, with electron density at the adduct site calculated using omit map ($F_o - F_c$) contoured at 2σ (Figure S3). This material is available free of charge via the Internet at http://pubs.acs.org.

Accession Codes

Complete structure factor data and final coordinates were deposited in the Protein Data Bank (www.rcsb.org): PDB ID codes for the ternary complexes of the HNE-dGuo adduct with dGTP for sequence I, 3T5H; and for sequence III, 3T5L; with dATP for sequence II, 3T5J; and for sequence IV, 3T5K.

■ AUTHOR INFORMATION

Corresponding Author

*Tel: 615-322-2589. Fax: 615-322-7591. E-mail: michael.p.stone@vanderbilt.edu.

Present Address

[†]Northeastern Collaborative Access Team and Department of Chemistry and Chemical Biology, Cornell University, Building 436E, Argonne National Laboratory, Argonne, IL 60439.

Funding

This work was supported by NIH Grants P01 ES-05355 (C.J.R., M.E., and M.P.S.), the Vanderbilt University Center in Molecular Toxicology, P30 ES-00267, and the Vanderbilt-Ingram Cancer Center, P30 CA-68485. Vanderbilt University and the Vanderbilt Center for Structural Biology assisted with the purchase of in-house crystallographic instrumentation. Crystallographic data were collected on the 21-ID-F beamline of the Life Sciences Collaborative Access Team (LS-CAT) at the Advanced Photon Source (Argonne National Laboratory, Argonne, IL). Supporting institutions may be found at http://ls-cat.org/members.html. Use of the Advanced Photon Source was supported by the U.S. Department of Energy, Basic Energy Sciences, Office of Science, under Contract W-31109-Eng-38.

■ ABBREVIATIONS

HNE, *trans*-4-hydroxynonenal; Dpo4, *Sulfolobus solfataricus* DNA polymerase IV; PdGuo, 1,N^2-propano-dGuo; M_1dGuo, 3-(2′-deoxy-β-D-erythro-pentofuranosyl)pyrimido[1,2-α]purin-10(3*H*)-one; LS-CAT, Life Science Collaborative Access Team

■ REFERENCES

(1) Benedetti, A., Comporti, M., and Esterbauer, H. (1980) Identification of 4-hydroxynonenal as a cytotoxic product originating from the peroxidation of liver microsomal lipids. *Biochim. Biophys. Acta 620*, 281−296.

(2) Esterbauer, H., Schaur, R. J., and Zollner, H. (1991) Chemistry and biochemistry of 4-hydroxynonenal, malonaldehyde and related aldehydes. *Free Radical Biol. Med. 11*, 81−128.

(3) Burcham, P. C. (1998) Genotoxic lipid peroxidation products: Their DNA damaging properties and role in formation of endogenous DNA adducts. *Mutagenesis 13*, 287−305.

(4) Lee, S. H., and Blair, I. A. (2000) Characterization of 4-oxo-2-nonenal as a novel product of lipid peroxidation. *Chem. Res. Toxicol. 13*, 698−702.

(5) Schneider, C., Tallman, K. A., Porter, N. A., and Brash, A. R. (2001) Two distinct pathways of formation of 4-hydroxynonenal. Mechanisms of nonenzymatic transformation of the 9- and 13-hydroperoxides of linoleic acid to 4-hydroxyalkenals. *J. Biol. Chem. 276*, 20831−20838.

(6) Schneider, C., Porter, N. A., and Brash, A. R. (2008) Routes to 4-hydroxynonenal: Fundamental issues in the mechanisms of lipid peroxidation. *J. Biol. Chem. 283*, 15539−15543.

(7) Parola, M., Bellomo, G., Robino, G., Barrera, G., and Dianzani, M. U. (1999) 4-Hydroxynonenal as a biological signal: Molecular basis and pathophysiological implications. *Antioxid. Redox Signaling 1*, 255−284.

(8) Poli, G., and Schaur, R. J. (2000) 4-Hydroxynonenal in the pathomechanisms of oxidative stress. *IUBMB Life 50*, 315−321.

(9) Nakashima, I., Liu, W., Akhand, A. A., Takeda, K., Kawamoto, Y., Kato, M., and Suzuki, H. (2003) 4-hydroxynonenal triggers multistep signal transduction cascades for suppression of cellular functions. *Mol. Aspects Med. 24*, 231−238.

(10) West, J. D., Ji, C., Duncan, S. T., Amarnath, V., Schneider, C., Rizzo, C. J., Brash, A. R., and Marnett, L. J. (2004) Induction of apoptosis in colorectal carcinoma cells treated with 4-hydroxy-2-nonenal and structurally related aldehydic products of lipid peroxidation. *Chem. Res. Toxicol. 17*, 453−462.

(11) West, J. D., and Marnett, L. J. (2005) Alterations in gene expression induced by the lipid peroxidation product, 4-hydroxy-2-nonenal. *Chem. Res. Toxicol. 18*, 1642−1653.

(12) West, J. D., and Marnett, L. J. (2006) Endogenous reactive intermediates as modulators of cell signaling and cell death. *Chem. Res. Toxicol. 19*, 173−194.

(13) Dwivedi, S., Sharma, A., Patrick, B., Sharma, R., and Awasthi, Y. C. (2007) Role of 4-hydroxynonenal and its metabolites in signaling. *Redox Rep. 12*, 4−10.

(14) Sayre, L. M., Zelasko, D. A., Harris, P. L., Perry, G., Salomon, R. G., and Smith, M. A. (1997) 4-Hydroxynonenal-derived advanced lipid peroxidation end products are increased in Alzheimer's disease. *J. Neurochem. 68*, 2092−2097.

(15) Yoritaka, A., Hattori, N., Uchida, K., Tanaka, M., Stadtman, E. R., and Mizuno, Y. (1996) Immunohistochemical detection of 4-hydroxynonenal protein adducts in Parkinson disease. *Proc. Natl. Acad. Sci. U.S.A. 93*, 2696−2701.

(16) Napoli, C., D'Armiento, F. P., Mancini, F. P., Postiglione, A., Witztum, J. L., Palumbo, G., and Palinski, W. (1997) Fatty streak formation occurs in human fetal aortas and is greatly enhanced by maternal hypercholesterolemia. Initial accumulation of low density lipoprotein and its oxidation precede monocyte recruitment into early atherosclerotic lesions. *J. Clin. Invest. 100*, 2680−2690.

(17) Yamagami, K., Yamamoto, Y., Kume, M., Ishikawa, Y., Yamaoka, Y., Hiai, H., and Toyokuni, S. (2000) Formation of 8-hydroxy-2′-deoxyguanosine and 4-hydroxy-2-nonenal-modified proteins in rat liver after ischemia-reperfusion: Distinct localization of the two oxidatively modified products. *Antioxid. Redox Signaling 2*, 127−136.

(18) Benamira, M., and Marnett, L. J. (1992) The lipid peroxidation product 4-hydroxynonenal is a potent inducer of the SOS response. *Mutat. Res. 293*, 1−10.

(19) Esterbauer, H., Eckl, P., and Ortner, A. (1990) Possible mutagens derived from lipids and lipid precursors. *Mutat. Res. 238*, 223−233.
(20) Eckl, P. M., Ortner, A., and Esterbauer, H. (1993) Genotoxic properties of 4-hydroxyalkenals and analogous aldehydes. *Mutat. Res. 290*, 183−192.
(21) Karlhuber, G. M., Bauer, H. C., and Eckl, P. M. (1997) Cytotoxic and genotoxic effects of 4-hydroxynonenal in cerebral endothelial cells. *Mutat. Res. 381*, 209−216.
(22) Eckl, P. M. (2003) Genotoxicity of HNE. *Mol. Aspects Med. 24*, 161−165.
(23) Emerit, I., Khan, S. H., and Esterbauer, H. (1991) Hydroxynonenal, a component of clastogenic factors? *Free Radical Biol. Med. 10*, 371−377.
(24) Winter, C. K., Segall, H. J., and Haddon, W. F. (1986) Formation of cyclic adducts of deoxyguanosine with the aldehydes *trans*-4-hydroxy-2-hexenal and *trans*-4-hydroxy-2-nonenal *in vitro*. *Cancer Res. 46*, 5682−5686.
(25) Douki, T., Odin, F., Caillat, S., Favier, A., and Cadet, J. (2004) Predominance of the 1,N^2-propano 2′-deoxyguanosine adduct among 4-hydroxy-2-nonenal-induced DNA lesions. *Free Radical Biol. Med. 37*, 62−70.
(26) Kowalczyk, P., Ciesla, J. M., Komisarski, M., Kusmierek, J. T., and Tudek, B. (2004) Long-chain adducts of *trans*-4-hydroxy-2-nonenal to DNA bases cause recombination, base substitutions and frameshift mutations in M13 phage. *Mutat. Res. 550*, 33−48.
(27) Xing, D. X., Sun, L. X., Cukier, R. I., and Bu, Y. X. (2007) Theoretical prediction of the p53 gene mutagenic mechanism induced by trans-4-hydroxy-2-nonenal. *J. Phys. Chem. B 111*, 5362−5371.
(28) Yi, P., Zhan, D., Samokyszyn, V. M., Doerge, D. R., and Fu, P. P. (1997) Synthesis and ^{32}P-postlabeling/high-performance liquid chromatography separation of diastereomeric 1,N^2-(1,3-propano)-2′-deoxyguanosine 3′-phosphate adducts formed from 4-hydroxy-2-nonenal. *Chem. Res. Toxicol. 10*, 1259−1265.
(29) Chung, F. L., Nath, R. G., Ocando, J., Nishikawa, A., and Zhang, L. (2000) Deoxyguanosine adducts of *t*-4-hydroxy-2-nonenal are endogenous DNA lesions in rodents and humans: Detection and potential sources. *Cancer Res. 60*, 1507−1511.
(30) Wacker, M., Schuler, D., Wanek, P., and Eder, E. (2000) Development of a ^{32}P-postlabeling method for the detection of 1,N^2-propanodeoxyguanosine adducts of *trans*-4-hydroxy-2-nonenal in vivo. *Chem. Res. Toxicol. 13*, 1165−1173.
(31) Wacker, M., Wanek, P., and Eder, E. (2001) Detection of 1,N^2-propanodeoxyguanosine adducts of *trans*-4-hydroxy-2-nonenal after gavage of *trans*-4-hydroxy-2-nonenal or induction of lipid peroxidation with carbon tetrachloride in F344 rats. *Chem.-Biol. Interact. 137*, 269−283.
(32) Chung, F. L., and Zhang, L. (2002) Deoxyguanosine adducts of *tert*-4-hydroxy-2-nonenal as markers of endogenous DNA lesions. *Methods Enzymol. 353*, 523−536.
(33) Liu, X., Lovell, M. A., and Lynn, B. C. (2006) Detection and quantification of endogenous cyclic DNA adducts derived from *trans*-4-hydroxy-2-nonenal in human brain tissue by isotope dilution capillary liquid chromatography nanoelectrospray tandem mass spectrometry. *Chem. Res. Toxicol. 19*, 710−718.
(34) Pan, J., Davis, W., Trushin, N., Amin, S., Nath, R. G., Salem, N. Jr., and Chung, F. L. (2006) A solid-phase extraction/high-performance liquid chromatography-based ^{32}P-postlabeling method for detection of cyclic 1,N^2-propanodeoxyguanosine adducts derived from enals. *Anal. Biochem. 348*, 15−23.
(35) Huang, H., Wang, H., Qi, N., Kozekova, A., Rizzo, C. J., and Stone, M. P. (2008) Rearrangement of the (6*S*,8*R*,11*S*) and (6*R*,8*S*,11*R*) exocyclic 1,N^2-deoxyguanosine adducts of *trans*-4-hydroxynonenal to N^2-deoxyguanosine cyclic hemiacetal adducts when placed complementary to cytosine in duplex DNA. *J. Am. Chem. Soc. 130*, 10898−10906.
(36) Feng, Z., Hu, W., Amin, S., and Tang, M. S. (2003) Mutational spectrum and genotoxicity of the major lipid peroxidation product, *trans*-4-hydroxy-2-nonenal, induced DNA adducts in nucleotide excision repair-proficient and -deficient human cells. *Biochemistry 42*, 7848−7854.
(37) Chung, F. L., Pan, J., Choudhury, S., Roy, R., Hu, W., and Tang, M. S. (2003) Formation of *trans*-4-hydroxy-2-nonenal- and other enal-derived cyclic DNA adducts from omega-3 and omega-6 polyunsaturated fatty acids and their roles in DNA repair and human p53 gene mutation. *Mutat. Res. 531*, 25−36.
(38) Choudhury, S., Pan, J., Amin, S., Chung, F. L., and Roy, R. (2004) Repair kinetics of *trans*-4-hydroxynonenal-induced cyclic 1,N^2-propanodeoxyguanine DNA adducts by human cell nuclear extracts. *Biochemistry 43*, 7514−7521.
(39) Chung, F. L., Komninou, D., Zhang, L., Nath, R., Pan, J., Amin, S., and Richie, J. (2005) Glutathione depletion enhances the formation of endogenous cyclic DNA adducts derived from *t*-4-hydroxy-2-nonenal in rat liver. *Chem. Res. Toxicol. 18*, 24−27.
(40) Falletti, O., Cadet, J., Favier, A., and Douki, T. (2007) Trapping of 4-hydroxynonenal by glutathione efficiently prevents formation of DNA adducts in human cells. *Free Radical Biol. Med. 42*, 1258−1269.
(41) Yadav, U. C., Ramana, K. V., Awasthi, Y. C., and Srivastava, S. K. (2008) Glutathione level regulates HNE-induced genotoxicity in human erythroleukemia cells. *Toxicol. Appl. Pharmacol. 227*, 257−264.
(42) Cajelli, E., Ferraris, A., and Brambilla, G. (1987) Mutagenicity of 4-hydroxynonenal in V79 Chinese hamster cells. *Mutat. Res. 190*, 169−171.
(43) Chung, F. L., Chen, H. J., Guttenplan, J. B., Nishikawa, A., and Hard, G. C. (1993) 2,3-epoxy-4-hydroxynonanal as a potential tumor-initiating agent of lipid peroxidation. *Carcinogenesis 14*, 2073−2077.
(44) Hussain, S. P., Raja, K., Amstad, P. A., Sawyer, M., Trudel, L. J., Wogan, G. N., Hofseth, L. J., Shields, P. G., Billiar, T. R., Trautwein, C., Hohler, T., Galle, P. R., Phillips, D. H., Markin, R., Marrogi, A. J., and Harris, C. C. (2000) Increased p53 mutation load in nontumorous human liver of Wilson disease and hemochromatosis: Oxyradical overload diseases. *Proc. Natl. Acad. Sci. U.S.A. 97*, 12770−12775.
(45) Hu, W., Feng, Z., Eveleigh, J., Iyer, G., Pan, J., Amin, S., Chung, F. L., and Tang, M. S. (2002) The major lipid peroxidation product, *trans*-4-hydroxy-2-nonenal, preferentially forms DNA adducts at codon 249 of human p53 gene, a unique mutational hotspot in hepatocellular carcinoma. *Carcinogenesis 23*, 1781−1789.
(46) Fernandes, P. H., Wang, H., Rizzo, C. J., and Lloyd, R. S. (2003) Site-specific mutagenicity of stereochemically defined 1,N^2-deoxyguanosine adducts of *trans*-4-hydroxynonenal in mammalian cells. *Environ. Mol. Mutagen. 42*, 68−74.
(47) Ling, H., Boudsocq, F., Woodgate, R., and Yang, W. (2001) Crystal structure of a Y-family DNA polymerase in action: A mechanism for error-prone and lesion-bypass replication. *Cell 107*, 91−102.
(48) Yang, W., and Woodgate, R. (2007) What a difference a decade makes: Insights into translesion DNA synthesis. *Proc. Natl. Acad. Sci. U.S.A. 104*, 15591−15598.
(49) Eoff, R. L., Egli, M., and Guengerich, F. P. (2010) Impact of chemical adducts on translesion synthesis in replicative and bypass polymerases: From structure to kinetics. In *The Chemical Biology of DNA Damage* (Geacintov, N. E., and Broyde, S., Eds.) pp 299−330, Wiley-VCH Verlag GmbH & Co. KGaA, Weinheim, Germany.
(50) Wang, H., Kozekov, I. D., Harris, T. M., and Rizzo, C. J. (2003) Site-specific synthesis and reactivity of oligonucleotides containing stereochemically defined 1,N^2-deoxyguanosine adducts of the lipid peroxidation product *trans*-4-hydroxynonenal. *J. Am. Chem. Soc. 125*, 5687−5700.
(51) Zang, H., Goodenough, A. K., Choi, J. Y., Irimia, A., Loukachevitch, L. V., Kozekov, I. D., Angel, K. C., Rizzo, C. J., Egli, M., and Guengerich, F. P. (2005) DNA adduct bypass polymerization by *Sulfolobus solfataricus* DNA polymerase Dpo4. Analysis and crystal structures of multiple base-pair substitution and frameshift products with the adduct 1,N^2-ethenoguanine. *J. Biol. Chem. 289*, 29750−29764.
(52) Wang, H., and Rizzo, C. J. (2001) Stereocontrolled syntheses of all four stereoisomeric 1,N^2-deoxyguanosine adducts of the lipid peroxidation product *trans*-4-hydroxynonenal. *Org. Lett. 3*, 3603−3605.

(53) Cavaluzzi, M. J., and Borer, P. N. (2004) Revised UV extinction coefficients for nucleoside-5′-monophosphates and unpaired DNA and RNA. *Nucleic Acids Res. 32*, e13.
(54) Otwinowski, Z., and Minor, W. (1997) Processing of X-ray diffraction data collected in oscillation mode. *Acta Crystallogr., Sect. A 276*, 307−326.
(55) French, S., and Wilson, K. (1978) Treatment of negative intensity observations. *Acta Crystallogr., Sect. A 34*, 517−525.
(56) Brunger, A. T., Adams, P. D., Clore, G. M., DeLano, W. L., Gros, P., Grosse-Kunstleve, R. W., Jiang, J. S., Kuszewski, J., Nilges, M., Pannu, N. S., Read, R. J., Rice, L. M., Simonson, T., and Warren, G. L. (1998) Crystallography & NMR system: A new software suite for macromolecular structure determination. *Acta Crystallogr., Sect. D: Biol. Crystallogr. 54*, 905−921.
(57) Vellieux, F. M. D., and Dijkstra, B. W. (1997) Computation of Bhat's OMIT maps with different coefficients. *J. Appl. Crystallogr. 30*, 396−399.
(58) Cambillau, C., and Roussel, A. (1997) *TURBO FRODO Version OpenGL.1*, Université Aix-Marseille II, Marseille, France
(59) DeLano, W. L. (2008) *The PyMOL Molecular Graphics System*, DeLano Scientific LLC, Palo Alto, CA.
(60) Irimia, A., Zang, H., Loukachevitch, L. V., Eoff, R. L., Guengerich, F. P., and Egli, M. (2006) Calcium is a cofactor of polymerization but inhibits pyrophosphorolysis by the *Sulfolobus solfataricus* DNA polymerase Dpo4. *Biochemistry 45*, 5949−5956.
(61) Irimia, A., Loukachevitch, L. V., Eoff, R. L., Guengerich, F. P., and Egli, M. (2010) Metal-ion dependence of the active-site conformation of the translesion DNA polymerase Dpo4 from *Sulfolobus solfataricus*. *Acta Crystallogr., Sect. F: Struct. Biol. Cryst. Commun. 66*, 1013−1018.
(62) Silvian, L. F., Toth, E. A., Pham, P., Goodman, M. F., and Ellenberger, T. (2001) Crystal structure of a DinB family error-prone DNA polymerase from *Sulfolobus solfataricus*. *Nat. Struct. Biol. 8*, 984−989.
(63) Nair, D. T., Johnson, R. E., Prakash, S., Prakash, L., and Aggarwal, A. K. (2004) Replication by human DNA polymerase-iota occurs by Hoogsteen base-pairing. *Nature 430*, 377−380.
(64) Eoff, R. L., Stafford, J. B., Szekely, J., Rizzo, C. J., Egli, M., Guengerich, F. P., and Marnett, L. J. (2009) Structural and functional analysis of *Sulfolobus solfataricus* Y-family DNA polymerase Dpo4-catalyzed bypass of the malondialdehyde-deoxyguanosine adduct. *Biochemistry 48*, 7079−7088.
(65) Wang, Y., Musser, S. K., Saleh, S., Marnett, L. J., Egli, M., and Stone, M. P. (2008) Insertion of dNTPs opposite the 1,N^2-propanodeoxyguanosine adduct by *Sulfolobus solfataricus* P2 DNA polymerase IV. *Biochemistry 47*, 7322−7334.
(66) Riggins, J. N., Daniels, J. S., Rouzer, C. A., and Marnett, L. J. (2004) Kinetic and thermodynamic analysis of the hydrolytic ring-opening of the malondialdehyde-deoxyguanosine adduct, 3-(2′-deoxy-beta-D-erythro-pentofuranosyl)- pyrimido[1,2-alpha]purin-10(3*H*)-one. *J. Am. Chem. Soc. 126*, 8237−8243.
(67) Riggins, J. N., Pratt, D. A., Voehler, M., Daniels, J. S., and Marnett, L. J. (2004) Kinetics and mechanism of the general-acid-catalyzed ring-closure of the malondialdehyde-DNA adduct, N^2-(3-oxo-1-propenyl)deoxyguanosine (N^2OPdG-), to 3-(2′-deoxy-beta-D-erythro-pentofuranosyl)pyrimido[1,2-alpha]purin-10(3*H*)-one (M_1dG). *J. Am. Chem. Soc. 126*, 10571−10581.
(68) DeCarlo, L., Gowda, A. S., Suo, Z., and Spratt, T. E. (2008) Formation of purine-purine mispairs by *Sulfolobus solfataricus* DNA polymerase IV. *Biochemistry 47*, 8157−8164.
(69) Marinelli, E. R., Johnson, F., Iden, C. R., and Yu, P. L. (1990) Synthesis of 1,N^2-(1,3-propano)-2′-deoxyguanosine and incorporation into oligodoexynucleotides: A model for exocyclic acrolein-DNA adducts. *Chem. Res. Toxicol. 3*, 49−58.
(70) Kouchakdjian, M., Marinelli, E., Gao, X., Johnson, F., Grollman, A., and Patel, D. (1989) NMR studies of exocyclic 1,N^2-propanodeoxyguanosine adducts (X) opposite purines in DNA duplexes: Protonated X(*syn*):A(*anti*) pairing (acidic pH) and X(*syn*):G(*anti*) pairing (neutral pH) at the lesion site. *Biochemistry 28*, 5647−5657.
(71) Kouchakdjian, M., Eisenberg, M., Live, D., Marinelli, E., Grollman, A. P., and Patel, D. J. (1990) NMR studies of an exocyclic 1,N^2-propanodeoxyguanosine adduct (X) located opposite deoxyadenosine (A) in DNA duplexes at basic pH: Simultaneous partial intercalation of X and A between stacked bases. *Biochemistry 29*, 4456−4465.
(72) Huang, P., and Eisenberg, M. (1992) The three-dimensional structure in solution (pH 5.8) of a DNA 9-mer duplex containing 1,N^2-propanodeoxyguanosine opposite deoxyadenosine. Restrained molecular dynamics and NOE-based refinement calculations. *Biochemistry 31*, 6518−6532.
(73) Huang, P., Patel, D. J., and Eisenberg, M. (1993) Solution structure of the exocyclic 1,N^2-propanodeoxyguanosine adduct opposite deoxyadenosine in a DNA nonamer duplex at pH 8.9. Model of pH-dependent conformational transition. *Biochemistry 32*, 3852−3866.
(74) Singh, U. S., Moe, J. G., Reddy, G. R., Weisenseel, J. P., Marnett, L. J., and Stone, M. P. (1993) ^{1}H NMR of an oligodeoxynucleotide containing a propanodeoxyguanosine adduct positioned in a $(CG)_3$ frameshift hotspot of *Salmonella typhimurium hisD3052*: Hoogsteen base-pairing at pH 5.8. *Chem. Res. Toxicol. 6*, 825−836.
(75) Weisenseel, J. P., Reddy, G. R., Marnett, L. J., and Stone, M. P. (2002) Structure of an oligodeoxynucleotide containing a 1,N^2-propanodeoxyguanosine adduct positioned in a palindrome derived from the *Salmonella typhimurium hisD3052* gene: Hoogsteen pairing at pH 5.2. *Chem. Res. Toxicol. 15*, 127−139.
(76) Haracska, L., Yu, S. L., Johnson, R. E., Prakash, L., and Prakash, S. (2000) Efficient and accurate replication in the presence of 7,8-dihydro-8-oxoguanine by DNA polymerase eta. *Nat. Genet. 25*, 458−461.
(77) Johnson, R. E., Washington, M. T., Haracska, L., Prakash, S., and Prakash, L. (2000) Eukaryotic polymerases iota and zeta act sequentially to bypass DNA lesions. *Nature 406*, 1015−1019.
(78) Johnson, R. E., Prakash, S., and Prakash, L. (2000) The human DINB1 gene encodes the DNA polymerase pol theta. *Proc. Natl. Acad. Sci. U.S.A. 97*, 3838−3843.
(79) Zhang, Y., Yuan, F., Wu, X., Rechkoblit, O., Taylor, J. S., Geacintov, N. E., and Wang, Z. (2000) Error-prone lesion bypass by human DNA polymerase eta. *Nucleic Acids Res. 28*, 4717−4724.
(80) Ohashi, E., Ogi, T., Kusumoto, R., Iwai, S., Masutani, C., Hanaoka, F., and Ohmori, H. (2000) Error-prone bypass of certain DNA lesions by the human DNA polymerase kappa. *Genes Dev. 14*, 1589−1594.
(81) Boudsocq, F., Iwai, S., Hanaoka, F., and Woodgate, R. (2001) *Sulfolobus solfataricus* P2 DNA polymerase IV (Dpo4): An archaeal DinB-like DNA polymerase with lesion-bypass properties akin to eukaryotic poleta. *Nucleic Acids Res. 29*, 4607−4616.
(82) Gerlach, V. L., Feaver, W. J., Fischhaber, P. L., and Friedberg, E. C. (2001) Purification and characterization of pol kappa, a DNA polymerase encoded by the human DINB1 gene. *J. Biol. Chem. 276*, 92−98.
(83) Frank, E. G., Sayer, J. M., Kroth, H., Ohashi, E., Ohmori, H., Jerina, D. M., and Woodgate, R. (2002) Translesion replication of benzo[*a*]pyrene and benzo[*c*]phenanthrene diol epoxide adducts of deoxyadenosine and deoxyguanosine by human DNA polymerase iota. *Nucleic Acids Res. 30*, 5284−5292.
(84) Rechkoblit, O., Zhang, Y., Guo, D., Wang, Z., Amin, S., Krzeminsky, J., Louneva, N., and Geacintov, N. E. (2002) trans-Lesion synthesis past bulky benzo[*a*]pyrene diol epoxide N^2-dG and N^6-dA lesions catalyzed by DNA bypass polymerases. *J. Biol. Chem. 277*, 30488−30494.
(85) Huang, X., Kolbanovskiy, A., Wu, X., Zhang, Y., Wang, Z., Zhuang, P., Amin, S., and Geacintov, N. E. (2003) Effects of base sequence context on translesion synthesis past a bulky (+)-*trans-anti*-B[a]P-N^2-dG lesion catalyzed by the Y-family polymerase pol kappa. *Biochemistry 42*, 2456−2266.

(86) Washington, M. T., Minko, I. G., Johnson, R. E., Wolfle, W. T., Harris, T. M., Lloyd, R. S., Prakash, S., and Prakash, L. (2004) Efficient and error-free replication past a minor-groove DNA adduct by the sequential action of human DNA polymerases iota and kappa. *Mol. Cell. Biol. 24*, 5687−5693.
(87) Washington, M. T., Minko, I. G., Johnson, R. E., Haracska, L., Harris, T. M., Lloyd, R. S., Prakash, S., and Prakash, L. (2004) Efficient and error-free replication past a minor-groove N^2-guanine adduct by the sequential action of yeast Rev1 and DNA polymerase zeta. *Mol. Cell. Biol. 24*, 6900−6906.
(88) Nair, D. T., Johnson, R. E., Prakash, L., Prakash, S., and Aggarwal, A. K. (2005) Human DNA polymerase iota incorporates dCTP opposite template G via a G:C + Hoogsteen base pair. *Structure 13*, 1569−1577.
(89) Nair, D. T., Johnson, R. E., Prakash, L., Prakash, S., and Aggarwal, A. K. (2006) An incoming nucleotide imposes an *anti* to *syn* conformational change on the templating purine in the human DNA polymerase-iota active site. *Structure 14*, 749−755.
(90) Nair, D. T., Johnson, R. E., Prakash, L., Prakash, S., and Aggarwal, A. K. (2006) Hoogsteen base pair formation promotes synthesis opposite the 1,N^6-ethenodeoxyadenosine lesion by human DNA polymerase iota. *Nat. Struct. Mol. Biol. 13*, 619−625.
(91) Wolfle, W. T., Johnson, R. E., Minko, I. G., Lloyd, R. S., Prakash, S., and Prakash, L. (2006) Replication past a *trans*-4-hydroxynonenal minor-groove adduct by the sequential action of human DNA polymerases iota and kappa. *Mol. Cell. Biol. 26*, 381−386.